

## Parameter Identification of Damage-based Hysteretic Model for Pipe-section Steel Bridge Piers

Qingyun Liu\*, Akira Kasai\*\*, Tsutomu Usami\*\*\*

\* M. of Eng., Graduate Student, Dept. of Civil Eng., Nagoya University, Chikusa-ku, Nagoya 464-8603

\*\* M. of Eng., Research Associate, Dept. of Civil Eng., Nagoya University, Chikusa-ku, Nagoya 464-8603

\*\*\* Dr. of Eng., Dr. of Sc., Professor, Dept. of Civil Eng., Nagoya University, Chikusa-ku, Nagoya 464-8603

The damage-based hysteretic restoring force model proposed by Kumar · Usami<sup>(1,2)</sup> is an effective tool in inelastic seismic response analysis and seismic damage evaluation of thin-walled steel bridge piers. Toward practical application of the damage index and the hysteretic model with pipe-section steel bridge piers, a method for systematically identifying the free parameters contained in the damage index is proposed, and relationship between the free parameters and structural parameters is clarified. Empirical equations for strength and ductility parameters are also given based on FEM analysis results. Finally, performance of the hysteretic model is illustrated by simulation of pseudodynamic tests of pipe-section steel bridge piers.

*Key words: damage index, hysteretic model, seismic, thin-walled, steel bridge piers*

### 1. Introduction

Thin-walled steel bridge piers find wide use in highway bridge structures in Japan. The structural characteristics of these bridge piers make them susceptible to damage in the form of local as well as overall interaction buckling and their hysteretic behavior is marked by relatively high rate of degradation in strength and stiffness. Based on cyclic loading tests of thin-walled steel box columns, a comprehensive damage index formulation has been proposed by Kumar · Usami for seismic damage evaluation of this type of structures<sup>1)</sup>. This damage index formulation combines the deformation-based and hysteretic energy-based damages, and forms the basis for the development of an evolutionary-degrading hysteretic restoring force model<sup>1)-3)</sup>. This damage-based hysteretic model proves to be capable of simulating pseudodynamic tests of thin-walled box columns. Toward practical application of the hysteretic model in seismic response analysis, there is a need to extend the damage index to steel bridge piers of other cross sections and to systematically determine the model parameters and in particular the free parameters ( $\beta$  and  $c$  in Eq.(1)) contained in the damage index expression. An attempt has been made by Kumar · Mizutani · Okamoto<sup>4)</sup> to apply the model to predict seismic response of pipe-section steel bridge piers. However, there is a drawback in their analyses: the values of the free parameters are unchanged from those for box-section columns. According to a study on the sensitivity of model performance to the values of the free parameters (Section 7 of this paper), cautions should be taken in choosing the free parameters since model performance is cumulative sensitive to the values of the free parameters especially the value of  $c$ . Thus systematic parameter identification is indispensable for extending the damage-based hysteretic model to seismic analysis of pipe-

section steel bridge piers.

Unlike other structural parameters, the free parameters have no concrete physical meanings; however, they play important analytical roles in damage evaluation. And since the damage-based hysteretic model relies heavily on damage evaluation, choice of the damage index parameters shall definitely affect performance of the damage-based hysteretic model. Main purpose of this study is to relate the free parameters to the basic structural parameters for pipe-section steel bridge piers thus overcoming arbitrariness in choosing the free parameters which is the major obstacle in applying the damage-based hysteretic model.

Based on experimental observations, the criterion of cyclic residual strength dropping to initial yield strength has been proposed for defining structural failure in the damage index formulation<sup>1)-4)</sup>. With this definition of collapse, a method for systematically evaluating the free parameters of the damage index providing realistic hysteretic curves is proposed in this study. The method is basically a numerical least-squares procedure aimed at selecting the statistically optimum system parameters. More importantly, this method opens the way to rationalize choice of the free parameters in the light of bringing the damage index close to unity at collapse.

Immediately following this introduction is a brief discussion on the damage index and the hysteretic model. Next, the parameter identifying method is presented. Applying this method, correlation between the damage index free parameters and basic structural parameters is then investigated for thin-walled pipe-section steel bridge piers. This investigation leads to simple equations for determining the free parameters. To further facilitate application, other structural parameters involved in the damage-based hysteretic model are also given in a series of empirical equations obtained from FEM analysis results. Finally, as an

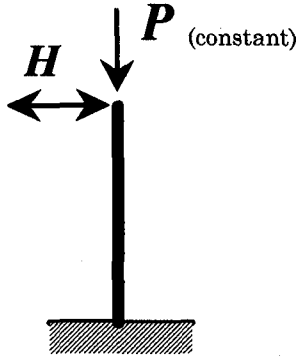


Fig.1 Modeling of single bridge pier

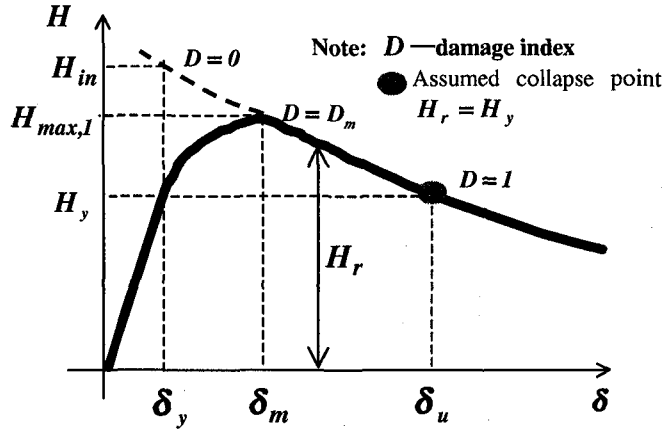


Fig.2 Degradation of strength (monotonic loading)

overall test on the success in this parameter identifying effort, inelastic seismic response analysis is carried out to simulate pseudodynamic tests on pipe-section steel bridge piers using the damage-based hysteretic model.

## 2. Damage index and the damage-based hysteretic model

### 2.1 Damage index formulation

Single bridge piers of cantilever type are usually idealized as single-degree-of-freedom system with the mass concentrated at the top. And in cyclic loading tests, specimens to model such bridge piers are usually tested as cantilever columns fixed at the base and subjected to a constant axial load and cyclic lateral loading at the free end (Fig.1). Based on cyclic tests of thin-walled box-section columns modeling thin-walled steel bridge piers, the following damage index has been proposed<sup>11</sup>:

$$D = (1 - \beta) \sum_{j=1}^{N_l} \left[ \left( \frac{\delta_{max,j} - \delta_y}{\delta_u - \delta_y} \right)^c \right] + \beta \sum_{i=1}^N \left[ \left( \frac{E_i}{H_y(\delta_u - \delta_y)} \right)^c \right] \quad (1)$$

wherein  $H_y$  and  $\delta_y$  are yield horizontal load and yield horizontal displacement respectively;  $\delta_u$  is the displacement at collapse under monotonic loading;  $\delta_{max,j}$  is maximum absolute displacement for the  $j$ -th half-cycle;  $N_l$  is the number of half-cycles producing  $\delta_{max,j}$  such that  $\delta_{max,j} > \delta_{max,j-1} + \delta_y$  and the initial reference  $\delta_{max,0}$  is designated as  $\delta_y$ ;  $E_i$  is the hysteretic energy absorbed during the  $i$ -th half-cycle;  $\beta$  and  $c$  are the two free parameters in this damage index formulation. It is evident that this damage index formulation is a mixed-type development from the deformation-based damage index model and plastic fatigue index definition; the first term considers the effect of large displacement, and the second term accounts for plastic low-cycle fatigue. From this damage index expression, it can be seen that the role of  $\beta$  is to specify the relative importance of deformation-based damage and hysteretic energy-based damage. And the parameter  $c$  has two major functions: firstly,  $c > 1.0$

gives relatively more importance to larger half-cycles; on the other hand, since it is the power to both the normalized half-cycle deformation and the normalized half-cycle hysteretic energy, it serves to relate damage under general cyclic condition to damage under simple monotonic condition.

Collapse state is defined as when the residual strength  $H_r$  (strength on the descending branch) drops to  $H_y$  as shown in Fig.2. By normalizing the deformation term and the plastic energy term in the damage index formulation, it is intended that the damage index always come to unity at collapse. At this point, it is worth noting that an easy-to-calculate quantity  $H_y(\delta_u - \delta_y)$  is used in the denominator of the second term instead of  $E_{mon}$  — the absorbed plastic energy up to collapse under monotonic loading (Fig.3(a)). Due to such a treatment, the damage index does not strictly come to unity at collapse under monotonic loading (i.e. when  $N_l = N = 1$ ;  $\delta_{max,j} = \delta_u$ ;  $E_i = E_{mon}$ ), but an analytical form of energy is still preferable for its simplicity. However, this error becomes increasingly larger with higher ductility in steel bridge piers as actual  $E_{mon}$  departs farther from  $H_y(\delta_u - \delta_y)$ . To bring the error to an acceptable level and at the same time keep the advantage of using an analytical quantity for normalizing the hysteretic energy, this study replaces  $H_y(\delta_u - \delta_y)$  with  $0.5(H_y + H_{max,1})(\delta_u - \delta_y)$  to normalize  $E_i$ , wherein  $H_{max,1}$  is the maximum strength reached under monotonic loading (see Fig.3(b)). With this modification, the expression for the damage index now becomes:

$$D = (1 - \beta) \sum_{j=1}^{N_l} \left[ \left( \frac{\delta_{max,j} - \delta_y}{\delta_u - \delta_y} \right)^c \right] + \beta \sum_{i=1}^N \left[ \left( \frac{E_i}{0.5(H_y + H_{max,1})(\delta_u - \delta_y)} \right)^c \right] \quad (2)$$

Fig.3 shows the physical meaning of  $H_y(\delta_u - \delta_y)$  and  $0.5(H_y + H_{max,1})(\delta_u - \delta_y)$ ; it is obvious that the latter comes closer to  $E_{mon}$ , thus with Eq.(2), the damage index under monotonic loading up to  $\delta_u$  comes satisfactorily close to unity whether the bridge pier under question is of

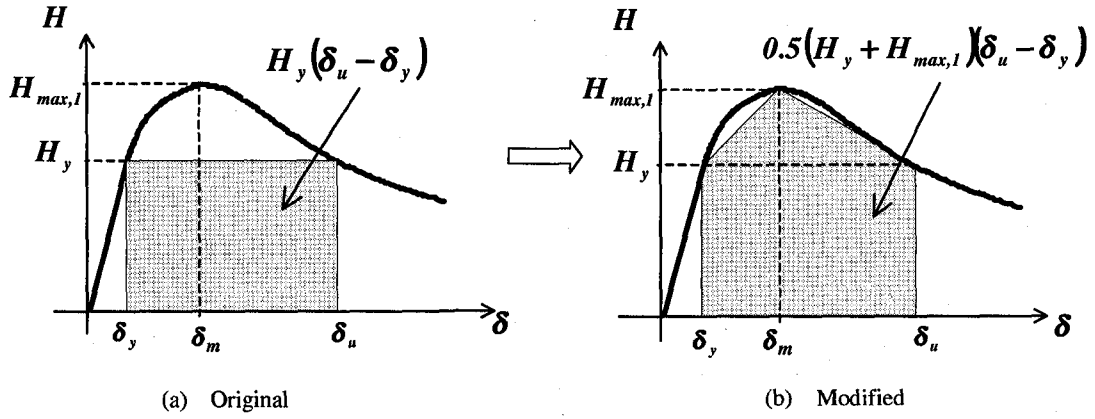
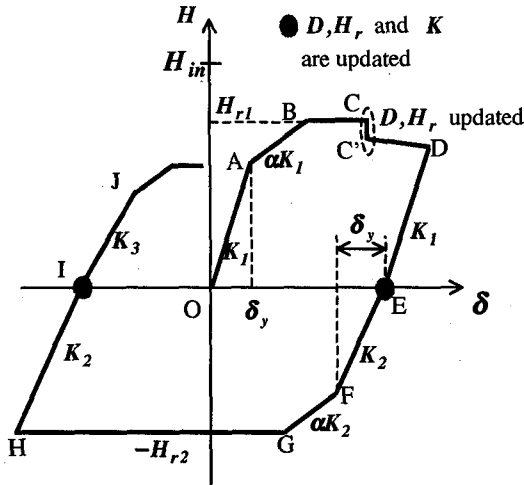


Fig.3 Physical meaning of the normalizing quantities for hysteretic energy (monotonic loading)



Note:  $K_2, K_3$  are calculated values of  $K$  by Eq.(4).

Fig.4 Damage-based hysteretic model

high-ductility class or not. Since  $H_{max,1}$  is also an inherent parameter in the damage-based hysteretic model, this modification does not add to the overall number of parameters.

## 2.2 The damage-based hysteretic model

Based on the above formulation of damage index, an evolutionary-degrading hysteretic restoring force model has also been developed<sup>(1,3)</sup>. Purpose of such a model is to simulate inelastic response of structure under dynamic loading by means of simplified hysteretic rules. The damage index forms the basis of this model in that degradation of strength and stiffness is prescribed as depending solely on damage index :

$$H_r = H_{in} \cdot \left(\frac{H_y}{H_{in}}\right)^D \quad (3)$$

$$K = K_1 \cdot \left(\frac{H_y}{H_{in}}\right)^D \quad (4)$$

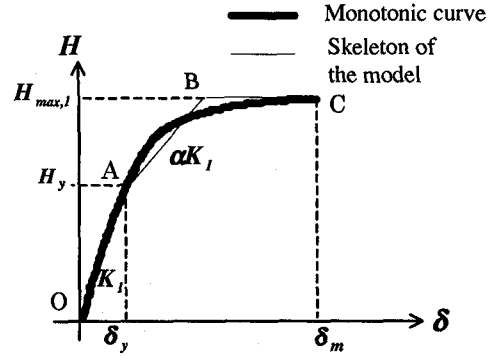


Fig.5 Evaluation of  $\alpha$

where  $D$  denotes the damage index;  $K_1$  is the initial elastic stiffness;  $H_{in}$  is the imaginary strength at  $D=0$ . See Fig.2 for an illustration of strength degradation from  $H_{in}$  to  $H_y$  at collapse under monotonic loading.

Calculation of  $H_{in}$  is as follows: first calculate the damage index value  $D_m$  (using Eq.(2)) at  $\delta = \delta_m$ ,  $H = H_{max,1}$  ( i.e. maximum loading point, see Fig.2); according to Eq.(3), there is  $H_{max,1} = H_{in} \cdot \left(\frac{H_y}{H_{in}}\right)^{D_m}$ , from which

$$H_{in} = \exp\left(\frac{\ln H_{max,1} - D_m \cdot \ln H_y}{1 - D_m}\right) \quad (5)$$

The hysteretic model is of piecewise multi-linear type. Basically the loading branch follows a tri-linear skeleton of an elastic limb, a hardening limb and a perfectly plastic limb. With updating of the damage index and residual strength, there may also be a descending limb in addition to the above three limbs. Fig.4 illustrates the loading and unloading rules of this model: The loading is initially elastic of stiffness  $K_1$  up to point A corresponding to a displacement of  $\delta_y$ ; From point A to point B, the strain hardening stiffness is  $\alpha$  times  $K_1$ ; The point B

corresponds to a load of  $H_{max} = H_r$ , and from point B, a perfectly plastic limb is followed until point C at which the damage index is updated and so is the residual strength; From point C and on, the loading follows a descending limb; Unloading from point D to point E is ruled to have the same stiffness as that of elastic loading OA; At the end of the first half cycle O-A-B-C-D-E, the damage index  $D$ , residual strength  $H_r$ , as well as elastic stiffness  $K$  are updated thus reloading in the opposite direction from point E to point F has the updated stiffness of  $K_2$ ; Point F corresponds to a displacement of  $\delta_y$  from point E; FG is another strain hardening limb with a stiffness of  $\alpha$  times  $K_2$ ; and a perfectly plastic limb follows point G and so on. It is ruled that  $D$ ,  $H_r$  and  $K$  be updated at the end of each half-cycle, but when to update  $D$  and  $H_r$  during a loading branch thus triggering a descending limb can be a matter of choice. Kumar · Usami suggested that  $D$  and  $H_r$  be updated at every increment of  $\delta_y$  during a particular half-cycle<sup>(1,2)</sup>. A simpler treatment is that they be updated whenever  $\delta_{max,j}$  exceeds the recorded maximum so far; in this case, there will be a significant increase in the damage index. And the latter is adopted in this study.

The parameter  $\alpha$  defines the ratio of hardening stiffness to elastic stiffness, and can be extracted from the monotonic  $H-\delta$  curve under an equal-energy principle<sup>3)</sup>, that is, in Fig.5, area under skeleton O-A-B-C should equal that under actual monotonic curve up to peak point C. It can be inferred that knowing  $\alpha$ ,  $\delta_m$  and  $H_{max,1}$ , with determined free parameters  $\beta$  and  $c$ , the damage index value  $D_m$  can be calculated, and in turn  $H_{in}$ . Hence  $D_m$  as well as  $H_{in}$  are taken as secondary quantities while  $\alpha$ ,  $\delta_m$  and  $H_{max,1}$  are deemed basic parameters of the model.

### 2.3 Model parameters

Given a certain thin-walled steel pier ( with definite size , material and axial force ratio ), the following parameters are needed in the damage-based hysteretic model:

- (1) Free parameters in the damage index —  $\beta$  and  $c$ ;
- (2)  $\delta_u$ ,  $H_{max,1}$ ,  $\delta_m$  and  $\alpha$ ; these parameters are to be extracted from the monotonic  $H-\delta$  curve.

In the practical design of thin-walled steel bridge piers of pipe section, three structural parameters are of major concern—radius-thickness ratio  $R_t$ , the slenderness ratio  $\bar{\lambda}$  and axial force ratio  $P/P_y$  ( $P_y$  is the squash load of the column cross section). The parameters  $R_t$  and  $\bar{\lambda}$  are defined as:

$$R_t = \sqrt{3(1-\nu^2)} \frac{\sigma_y D}{E 2t} \quad (6)$$

$$\bar{\lambda} = \frac{2h}{r} \frac{1}{\pi} \sqrt{\frac{\sigma_y}{E}} \quad (7)$$

wherein  $\sigma_y$  is yield stress of steel;  $E$  is Young's modulus;  $\nu$  is Poisson's ratio;  $D$  and  $t$  are diameter and thickness of the cross section respectively;  $h$  is column height and  $r$  radius of gyration of the cross section.

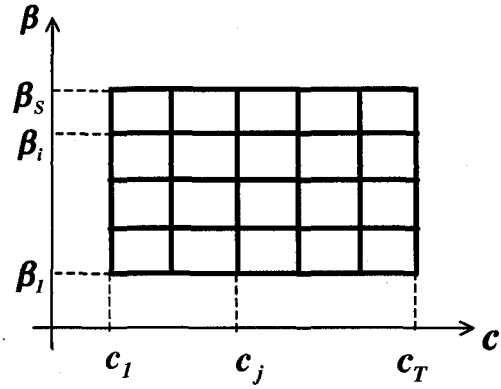


Fig.6 Selected grid in  $\beta - c$  space

For the damage-based hysteretic model to enter practical application, the above model parameters must be related to the three basic structural parameters and be related as simply as possible.

### 3. Method for identifying free parameters — $\beta$ and $c$

It is evident that evaluation of damage is pivotal to the hysteretic model. In particular, when  $D=1$ , the strength of the bridge pier according to Eq.(3) comes to:

$$H_{max} = H_{in} \cdot \left( \frac{H_y}{H_{in}} \right) = H_y, \text{ which means the structure has}$$

reached the assumed collapse point. For the model to faithfully reflect the real hysteretic behavior of the structure, it is essential that the two free parameters should bring the damage index close to unity at collapse under general cyclic loading conditions. Note that it is unnecessary and also impossible to have the damage index strictly come to unity at collapse because of imperfection of the damage index model—it takes into account only the major factors and neglects minor ones for sake of simplicity. Therefore, the damage index actually comes higher or lower than unity at collapse. In the light of this, statistical approach is most appropriate in calibrating  $\beta$  and  $c$ .

Given a definite steel bridge pier ( characterized by  $R_t$ ,  $\bar{\lambda}$ , and axial load ratio  $P/P_y$  ), and supplied with analysis results or test data under both monotonic and various cyclic loading paths up to collapse ( in the form of Horizontal force —Horizontal displacement curve), determination of  $\beta$  and  $c$  can be regarded as a nonlinear parameter estimation problem in the field of mathematical statistics. Desired  $\beta$  and  $c$  are those that would make the value of damage index closest to 1.0 at collapse for all kinds of cyclic loading paths. Note that  $H_y$ ,  $\delta_y$ ,  $\delta_u$ ,  $H_{max,1}$  can be viewed as constants in this parameter estimation problem since they are deterministic functions of  $R_t$ ,  $\bar{\lambda}$ , and  $P/P_y$ . Suppose a total number of  $M$  cyclic  $H-\delta$  curves are available. Overall deviation of the damage index at failure from unity can be measured by the following error sum of squares ( heretofore referred to as deviation of damage index ):

$$S(\beta, c) = \sum_{u=1}^M [D_u(\beta, c) - 1.0]^2 \quad (8)$$

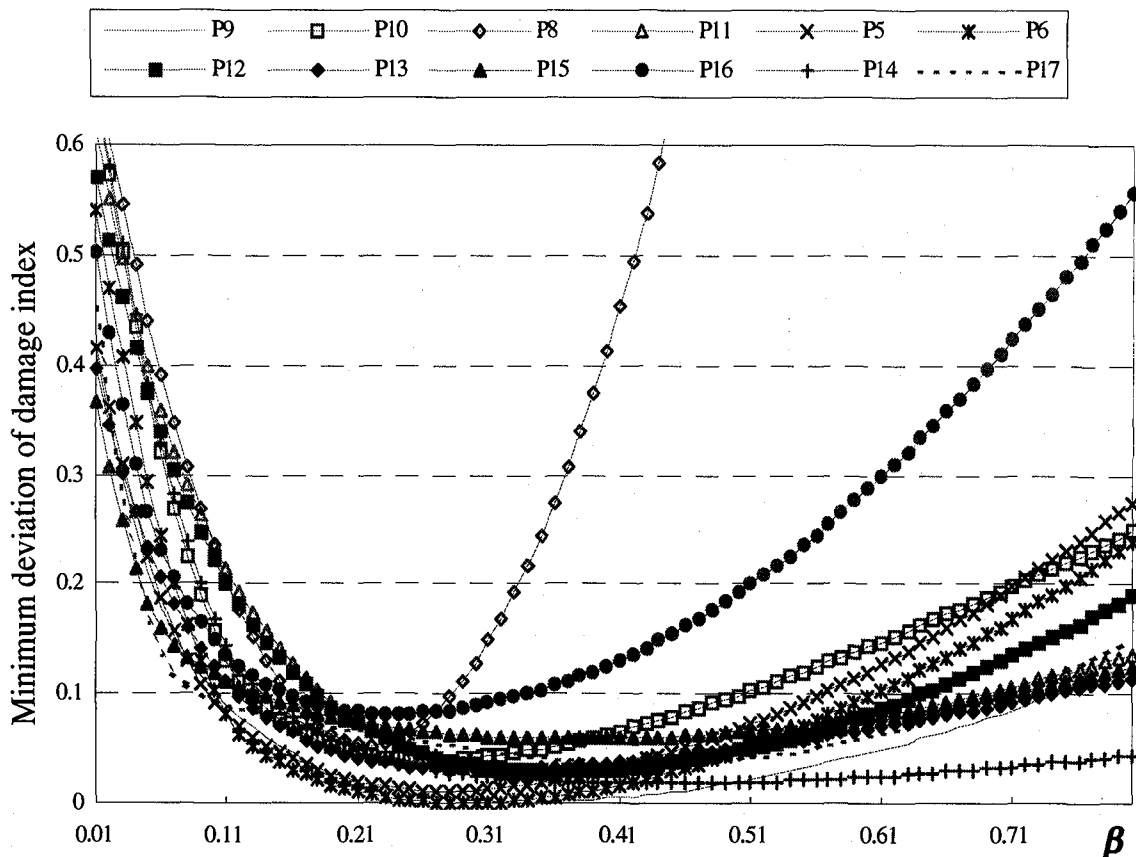


Fig.7 Local minimum deviation of damage index associated with  $\beta$   
 (Note: each plotted point marks the lowest deviation of damage index that is reached under a certain  $\beta$ ; Different curves correspond to different bridge piers.)

wherein  $D_u$  is the calculated value of damage index at collapse under the  $u$ -th cyclic loading path and shall be a function of  $\beta$  and  $c$ . With the aid of a computer, this parameter estimation problem can easily be solved by the following grid-and-plot procedure(Fig.6):

- (1) Select a grid of points in  $\beta$ - $c$  space. Make sure the interval of the grid suit the precision need for the two parameters and the grid cover the possible variation range of these two parameters.
- (2) Evaluate the deviation of damage index at every point of the grid. Desired values  $\beta$  and  $c$  then can easily identified by comparing deviation of damage index.

From a pure mathematical point of view, when two different hysteretic curves are available, two simultaneous equations can be formulated and solved for the two parameters, but the  $\beta, c$  values obtained in such a way is not necessarily the statistically optimum parameters in view of inevitable imperfection of the damage index model. Thus a statistical approach to obtain  $\beta, c$  requires a minimum number of three cyclic  $H-\delta$  curves for a particular bridge pier.

#### 4. Determination of free parameters for pipe-section steel bridge piers

As suggested by the above parameter identifying method,

calibration of  $\beta$  and  $c$  requires knowing the real hysteretic behavior of the structure. It has already been established that FEM analysis equipped with realistic constitutive law can predict very accurately cyclic behavior of thin-walled steel bridge piers<sup>5)</sup>, and numerical study has the advantage of flexibility in structural parameter selection. In this study, general purpose FEM program ABAQUS<sup>6)</sup> is used to generate hysteretic curves for a series of pipe-section steel bridge piers with different structural parameters. An accurate plasticity model – the two-surface model for structural steels with yield plateau<sup>7)</sup> is employed in the analysis. Details of the large-deformation inelastic analysis can be found in Ref. 5).

Structural parameters for the analyzed piers are listed in Table 1. Note that most of them have the same axial load ratio of 0.15 but varying  $R_t, \bar{\lambda}$ , and P5, P9, P11, P16 series are intended to study the effect of axial load ratio on the free parameters. For each of these piers,  $H-\delta$  curves are obtained under monotonic loading and three types of cyclic loading path: 1) Increasing-amplitude one-cycle loading (1-cycle); 2) Three-cycle loading (3-cycle); and 3) Constant-amplitude loading with one large first cycle (CA-L). These three types of cyclic loading path are considered to be representative in damage progression: Under 1-cycle, both deformation-based

**Table 1** Structural parameters of analyzed piers

Pier	$R_t$	$\bar{\lambda}$	$P/P_y$	Remarks
P1	0.050	0.20	0.15	
P2	0.075	0.20	0.15	
P3	0.088	0.20	0.15	
P4	0.110	0.20	0.15	
P5-10	0.075	0.25	0.10	P5 Series
P5-15	0.075	0.25	0.15	
P5-20	0.075	0.25	0.20	
P5-30	0.075	0.25	0.30	
P6	0.088	0.25	0.15	
P7	0.110	0.25	0.15	
P8	0.050	0.30	0.15	
P9-10	0.075	0.30	0.10	P9 Series
P9-15	0.075	0.30	0.15	
P9-20	0.075	0.30	0.20	
P9-30	0.075	0.30	0.30	
P10	0.088	0.30	0.15	
P11-10	0.110	0.30	0.10	P11 Series
P11-15	0.110	0.30	0.15	
P11-20	0.110	0.30	0.20	
P11-30	0.110	0.30	0.30	
P12	0.075	0.35	0.15	
P13	0.088	0.35	0.15	
P14	0.110	0.35	0.15	
P15	0.075	0.50	0.15	
P16-10	0.088	0.50	0.10	P16 Series
P16-15	0.088	0.50	0.15	
P16-20	0.088	0.50	0.20	
P16-30	0.088	0.50	0.30	
P17	0.110	0.50	0.15	

**Table 4** Deviation of damage index using Eq.(7) to get  $c$  ( $\beta=0.27$ )

$P/P_y=0.15$				
$R_t$	0.050	0.075	0.088	0.110
0.20	0.1125	0.0357	0.0226	0.0126
0.25		0.0167	0.0124	0.0040
0.30	0.1400	0.0062	0.0588	0.0427
0.35		0.0431	0.0508	0.0781
0.50		0.0729	0.0845	0.0585
Piers	$P/P_y$			
	0.10		0.20	0.30
P5	0.0185		0.0260	0.0504
P9	0.0035		0.1270	0.0052
P11	0.0600		0.0636	0.0925
P14	0.0598		0.3224	0.2226

damage and plastic energy-based damage increase from cycle to cycle; 3-cycle loading differs from 1-cycle in that repetition of each cyclic amplitude gives more weight to energy-based damage; Under CA-L, deformation-based damage occurs only in first cycle, afterwards only plastic energy based damage.

**Table 2** Best values of  $c$  with  $\beta=0.27$  ( $P/P_y=0.15$ )

$R_t$	0.050	0.075	0.088	0.110
0.20	1.37	1.28	1.25	1.30
0.25		1.31	1.29	1.36
0.30	1.56	1.40	1.32	1.40
0.35		1.54	1.61	1.37
0.50		1.70	1.76	1.82

**Table 3** Best values of  $c$  with  $\beta=0.27$  (Effect of axial load ratio)

Piers	$P/P_y$			
	0.10	0.15	0.20	0.30
P5	1.36	1.31	1.42	1.39
P9	1.40	1.40	1.57	1.44
P11	1.52	1.40	1.28	1.34
P14	1.69	1.76	1.84	1.90

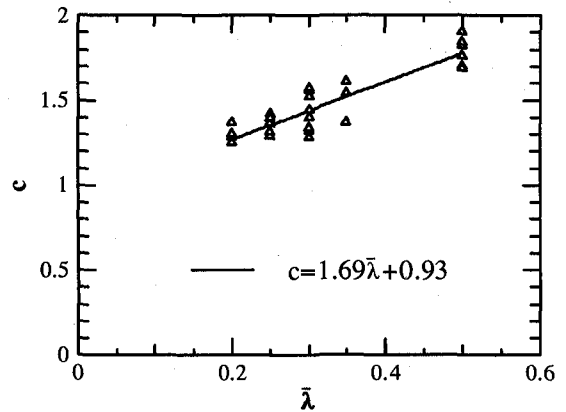


**Fig.8** Dependence of  $c$  on  $\bar{\lambda}$

Since the role of  $\beta$  is to specify the relative importance of deformation-based damage and plastic-energy-based damage, variation of  $S(\beta, c)$  with  $\beta$  is studied first. Based on the above grid-and-plot procedure, it is possible to find a local minimum deviation of damage index associated with a certain  $\beta$  value, that is,  $c$  is allowed to vary in giving the local minimum for each  $\beta$ . Plotting these local minimum deviation values using  $\beta$  as the abscissa,  $\beta$  values associated with the global minimum deviation can be identified for each bridge piers. It is found that irrespective of differing structural parameters, the global minimum deviation comes around  $\beta=0.20-0.30$  (Fig.7). In other words, global minimum of deviations are rather concentrated at this particular  $\beta$  interval. This fact justifies a fixed  $\beta$  value for all thin-walled pipe-section steel bridge piers of normal structural parameters. From analyzing the numerical results obtained in this study,  $\beta$  is fixed at 0.27 where overall local minimum deviation for all the analyzed piers becomes lowest.

With a fixed value of  $\beta$ , it is just logical to assign the

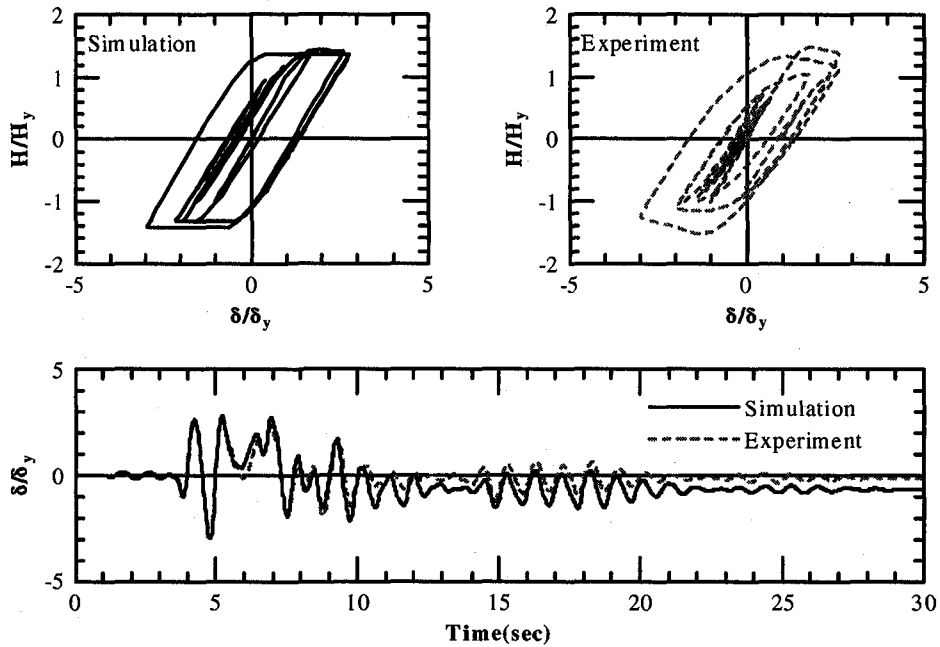


Fig.9 Response of TS11-30-16 to JMA accelerogram

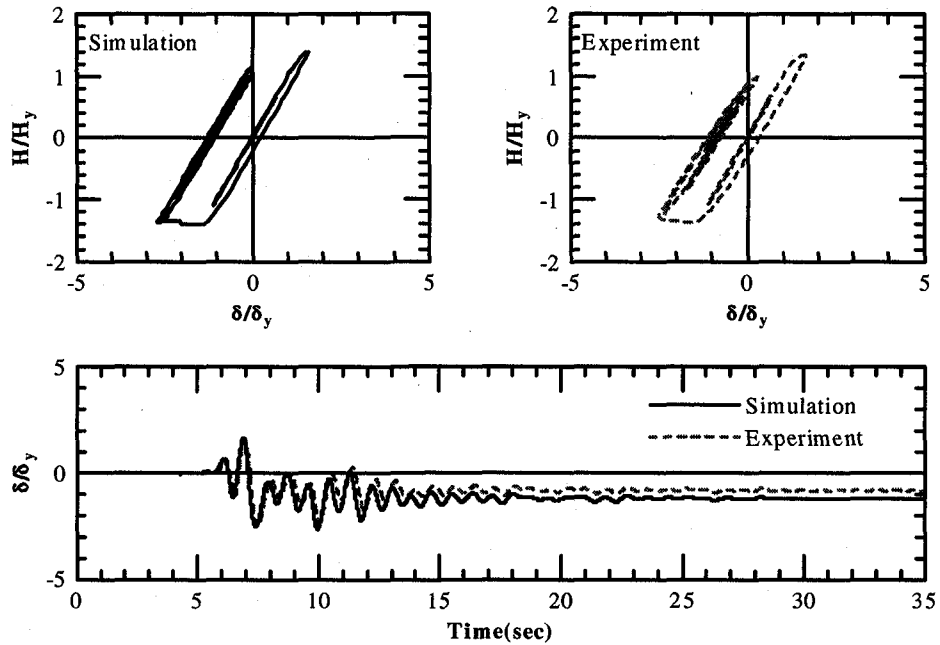


Fig.10 Response of TS11-30-11 to HKB accelerogram

very  $c$  that corresponds to the local minimum deviation at  $\beta=0.27$  to each bridge pier. Note that although these values resulted are still acceptably low since deviation of damage index has already got controlled in fixing  $\beta$ . Table 2 gives of  $c$  paired with  $\beta=0.27$  do not necessarily give the global minimum deviation of damage index, the deviations such best values of  $c$  for all the analyzed piers with axial load ratio of 0.15. From Table 2, it is evident that with the same  $\bar{\lambda}$ , there is only random fluctuation of  $c$  with

change in  $R_t$ , while there is a definite trend of  $c$  becoming higher with larger  $\bar{\lambda}$ . Also under  $\beta=0.27$ , investigation into variation of best  $c$  values with axial load ratio is summarized in Table 3. With identical structural parameters of  $R_t$  and  $\bar{\lambda}$ , there seems to be only slight random fluctuation of  $c$  under different axial load ratios, while it can surely be said that increasing in  $\bar{\lambda}$  results in a definite increase in  $c$  (note Table 3 is in increasing  $\bar{\lambda}$

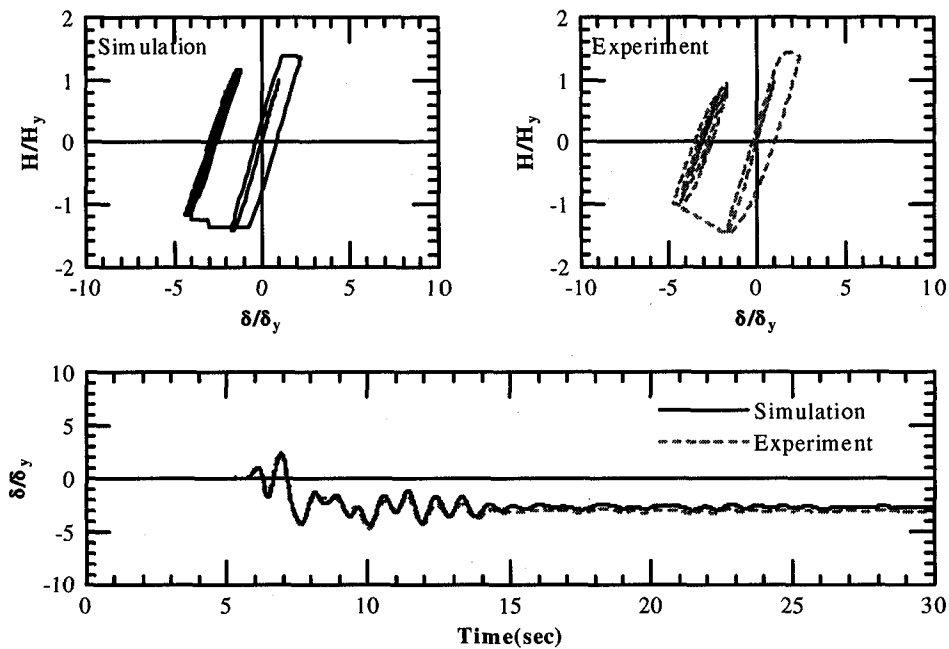


Fig.11 Response of TS11-30-11 to  $1.5 \times$  HKB accelerogram

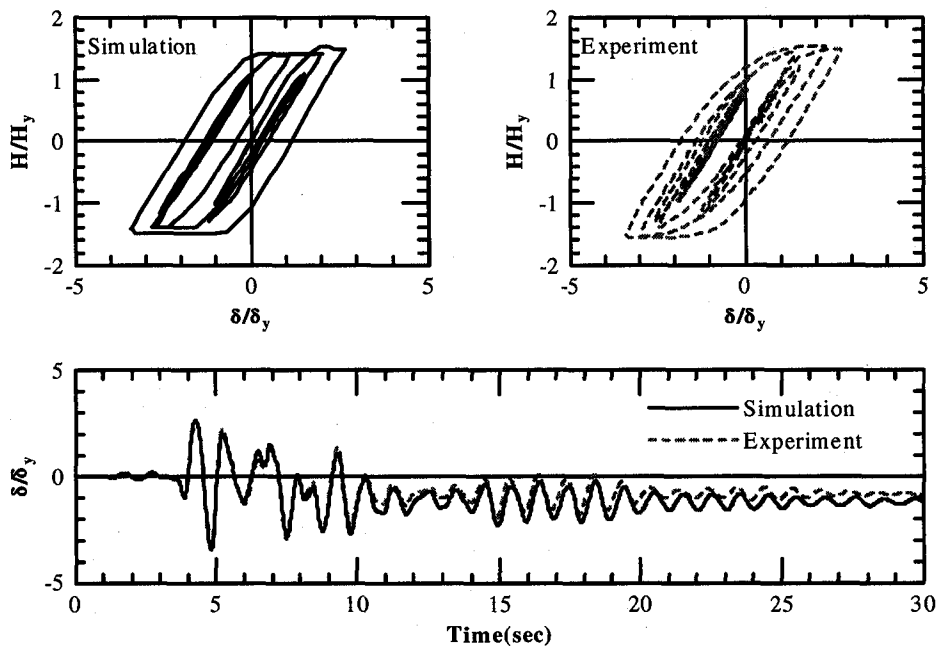


Fig.12 Response of TS08-30-18 to JMA accelerogram

order, P9 and P11 series have the same  $\bar{\lambda}$  of 0.30). Combining the results listed in Table 2 and Table 3, dependence of  $c$  on  $\bar{\lambda}$  can readily be summarized by a linear equation (Fig.8):

$$c = 1.69\bar{\lambda} + 0.93 \quad (0.20 \leq \bar{\lambda} \leq 0.50) \quad (9)$$

Using the approximate equation to get  $c$  combined with  $\beta = 0.27$ , the deviation of damage index for the analyzed piers are listed in Table 4. It can be said that the performance of the proposed equation for  $c$  combined with

fixed  $\beta$  of 0.27 is quite satisfactory.

It is worthwhile to point out that such simple rather than convoluted statistical correlation between the free parameters of the damage index and the structural parameters should come as no surprise. Of course, damageability of the structure has a lot to do with the structural parameters, but the free parameters are not directly related with damageability of the structure:  $\beta$  allots the two forms of damages and  $c$  relates damage under general seismic loading with the damage under simple monotonic



condition. In other words, values of the free parameter do not represent the very damageability of the structure. Hence it can also be rationalized that monotonic deformation and energy used as normalizing quantities in the damage index are significant in damage evaluation and performance of the hysteretic model. Monotonic loading parameters involved in the damage-based hysteretic model are addressed in the next section.

### 5. Monotonic loading parameters

As pointed out in section 2.3, apart from free parameters  $\beta$  and  $c$ , other parameters of the damage-based hysteretic model are extracted from monotonic  $H-\delta$  curve of the steel bridge pier. Based on large-deformation inelastic FEM analysis with ABAQUS program, these parameters are also given as functions of the basic structural parameters (See Appendix, Eqs.(A1)-(A4)).

### 6. Simulation of pseudo-dynamic tests

In this section, time-history analysis is carried out to simulate pseudo-dynamic tests on pipe-section steel bridge piers<sup>8)</sup>. The single bridge piers of cantilever type are modeled as SDOF system in the inelastic seismic response

analysis. Input earthquake excitations are two accelerograms of Hyogoken-Nanbu earthquake of January 17, 1995: one was recorded by Japan Meteorological Agency (JMA) ( NS component , ground type I ) and the other was observed at Higashi Kobe Bridge ( HKB ) ( NS component, ground type III ). The linear acceleration method (time interval:  $\Delta t = 0.02$  with JMA and  $\Delta t = 0.01$  with HKB) is used to solve the equation of motion with the restoring force given by the damage-based hysteretic model. Damping ratio is assumed as 0.05 . Structural parameters of the analyzed specimens are listed in Table 5. Parameters of the hysteretic model are calculated according to the empirical equations obtained in this study and are also listed in Table 5. Table 6 lists major analysis results in comparison with the test results. The predicted dynamic responses are compared with test results in Figs.9-12. Hysteretic loops predicted by the model show strong correlation with those from the tests, and maximum and minimum displacement show very good agreement with experimental results. Although there are occasionally noticeable discrepancies in residual displacement, it can still be said the damage-based hysteretic model is an effective and adequate tool considering many uncertainties about inelastic seismic response analysis.

**Table 5** Structural parameters of pseudodynamic test specimens

Test specimen (Accelerogram)	$R_t$	$\bar{\lambda}$	$P/P_y$	Mass ( $kN \cdot s^2 / mm$ )	$H_y$ (kN)	$\delta_y$ (mm)	$\alpha$	$\beta$	$c$	$H_{max,I}$	$\delta_u / \delta_y$	$\delta_m / \delta_y$
										$H_y$		
TS11-30-16(JMA)	0.102	0.316	0.155	1.84	$5.34 \times 10^3$	59.4	0.676	0.27	1.46	1.41	8.33	2.15
TS11-30-11(HKB)	0.119	0.338	0.111	1.48	$6.27 \times 10^3$	71.1	0.752	0.27	1.50	1.37	6.62	1.72
TS11-30-11 (1.5×HKB)	0.117	0.337	0.111	1.49	$6.31 \times 10^3$	70.7	0.744	0.27	1.50	1.37	6.82	1.76
TS08-30-18(JMA)	0.081	0.318	0.181	2.75	$6.59 \times 10^3$	58.0	0.585	0.27	1.47	1.46	11.6	3.06

Note: Mass,  $H_y$  and  $\delta_y$  have been converted to those of the assumed real bridge piers (scale factor=8.0)

**Table 6** Comparison of Test and Analysis results

Test specimen (Accelerogram)	$\delta_{max} / \delta_y$			$\delta_R / \delta_y$			$D$		
	Analysis (1)	Test (2)	(1)/(2)	Analysis (1)	Test (2)	(1)/(2)	Analysis (1)	Test (2)	(1)/(2)
TS11-30-16(JMA)	2.98	2.96	1.01	-0.67	-0.14	4.79	0.29	0.33	0.88
TS11-30-11(HKB)	2.69	2.47	1.09	-1.21	-0.82	1.48	0.10	0.075	1.33
TS11-30-11 (1.5×HKB)	4.38	4.69	0.93	-2.74	-3.10	0.88	0.53	0.53	1.00
TS08-30-18(JMA)	3.42	3.39	1.01	-1.25	-0.85	1.47	0.25	0.24	1.04

$\delta_{max}$  : maximum response displacement;  $\delta_R$  : residual displacement;  $D$  : damage index

### 7. Sensitivity of model performance to free parameters

This analytical study is aimed at investigating the effect of the values of free parameters on computed seismic response with the damage-based hysteretic model. Using different values of  $\beta$  and  $c$ , the responses of pipe-section steel bridge pier TS08-30-18 (structural parameters listed in Table 5) to two representative earthquake accelerograms are examined. Both are spectrum-fit accelerograms of Level 2 specified in JRA Specification<sup>9)</sup>:

1) ITAJIMA (maximum acceleration: 362.6 gal)–Level 2,

Type I, Ground type II accelerogram;

2) JR-Takatori, N-S component (maximum acceleration: 686.8 gal)–Level 2, Type II, Ground type II accelerogram modified from the record of Japan Railway Technical Research Institute near JR Takatori station during Hyogoken-Nanbu Earthquake of 1995.

Two values of  $\beta$  are employed: 0.27 obtained in this study and 0.11 used by Kumar et al.<sup>4)</sup>; a series values of  $c$ : 1.0, 1.2, 1.5, 2.0 paired with the two  $\beta$  values are used in the analyses.

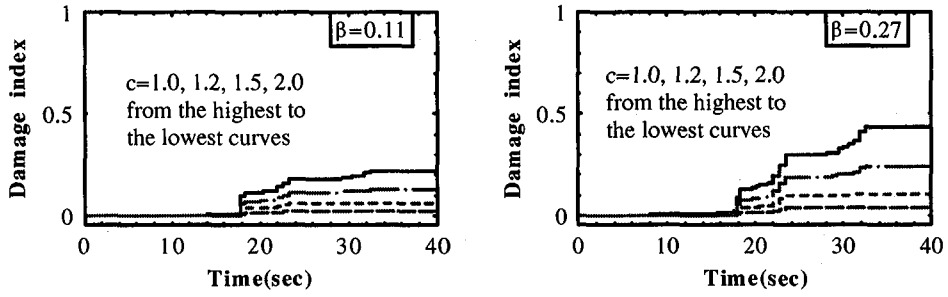


Fig.13 Damage progression under ITAJIMA

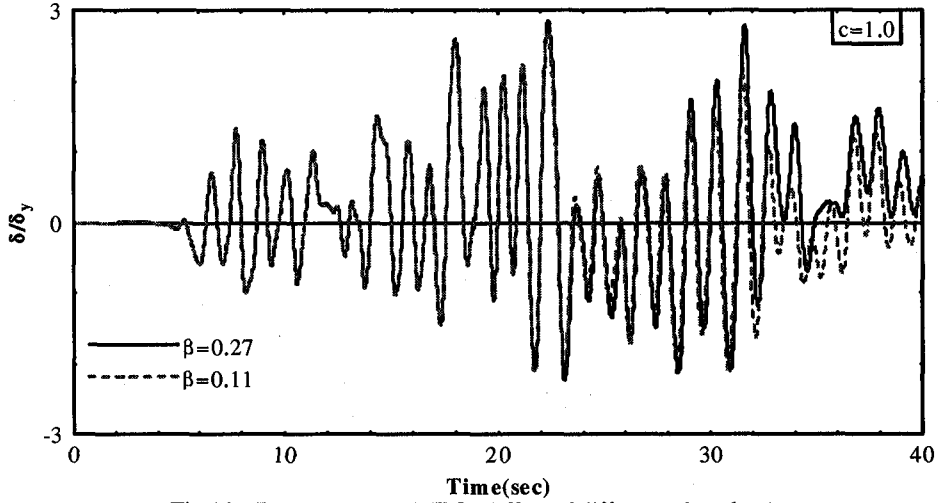


Fig.14 Responses to ITAJIMA (effect of different  $\beta$  values)

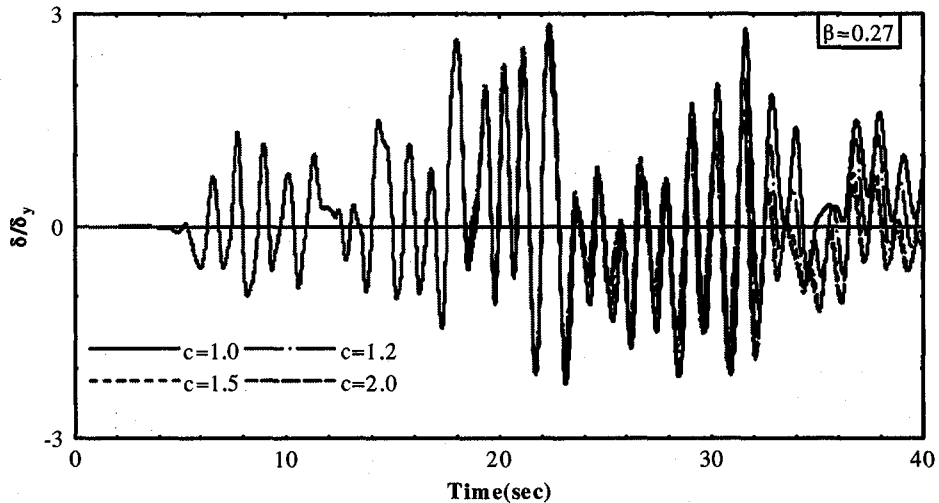


Fig.15 Responses to ITAJIMA (effect of different  $c$  values)

### 7.1 Responses to ITAJIMA accelerogram

Progression of the damage index under different combinations of  $\beta$  and  $c$  is shown in Fig.13. It can be seen that calculated damage to the structure is generally insignificant with all combinations of the free parameters ( $D_{final} < 0.5$ ), and patterns of damage index progression are all quite similar. As is expected from the formulation of the damage index, with the same  $\beta$  value,

the calculated damage index is lower with higher values of  $c$ . With the same  $c$  values, calculated damage with  $\beta = 0.27$  is always higher than with  $\beta = 0.11$ . That is because a larger  $\beta$  gives more weight to hysteretic energy-based damage, and energy-based damage is the frequent case while deformation-based damage is a relatively rare occurrence according to the damage index formulation.

It is found that at such a low damage level, difference in

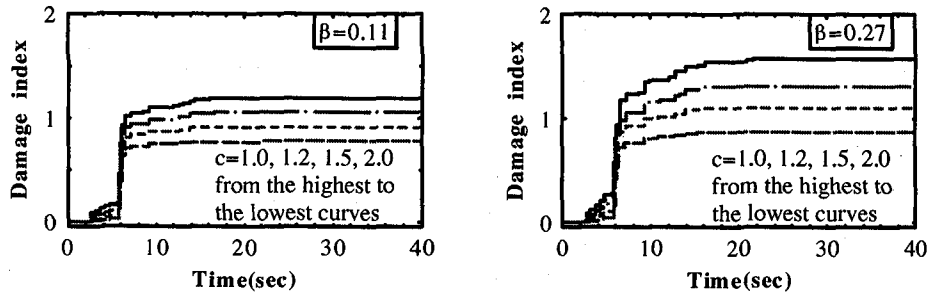


Fig.16 Damage progression under JR-Takatori

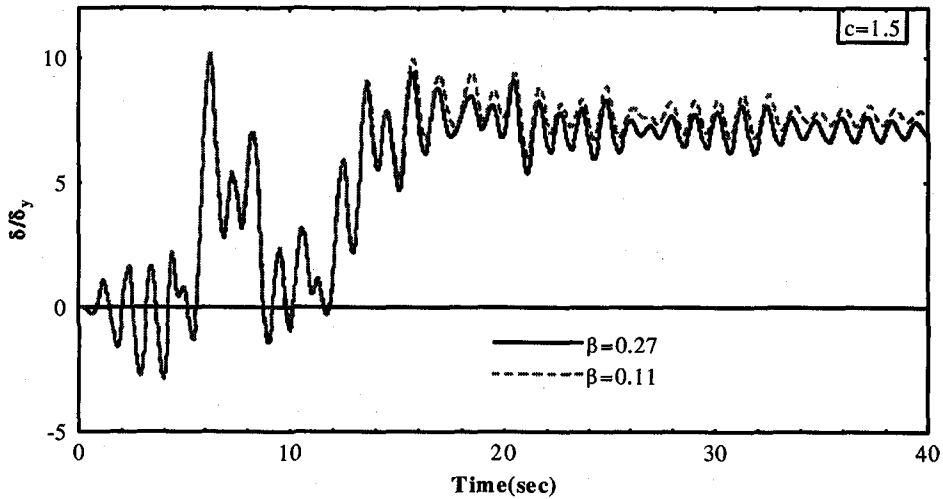


Fig.17 Responses JR-Takatori (effect of different  $\beta$  values)

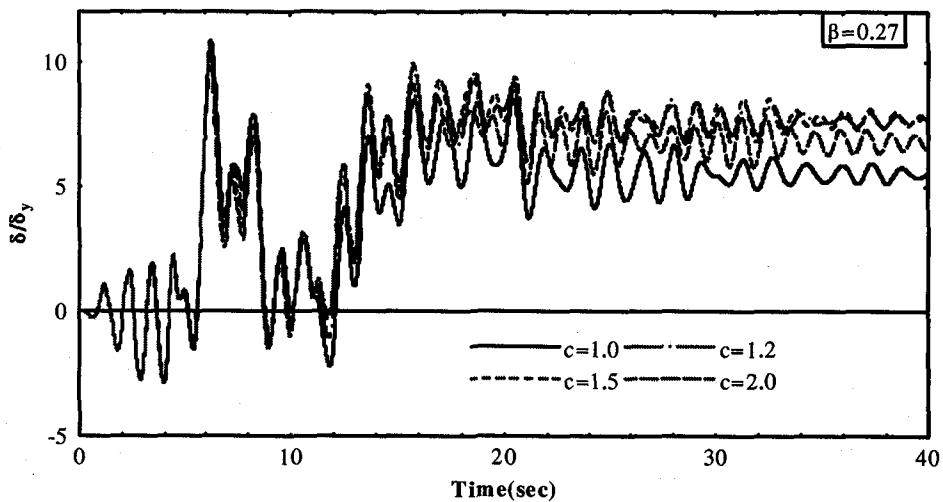


Fig.18 Responses to JR-Takatori (effect of different  $c$  values)

calculated displacement response under the two different  $\beta$  values is negligible if the value of  $c$  employed is the same. Fig.14 compares the responses under the two  $\beta$  values paired with the same  $c=1.0$ , and the difference is still less conspicuous with other  $c$  values. On the other hand, the same  $\beta$  value paired with different  $c$  values produces noticeable difference in response. Fig.15 gives the responses with different  $c$  values under the same  $\beta=0.27$ . Besides,

difference in response, just like the progression of damage, seems to be cumulative: during the earlier cycles, calculated responses with different  $c$  values almost coincide with each other, while they go separate ways as the difference in calculated damage becomes larger.

### 7.2 Responses to JR-Takatori accelerogram

Progression of damage is shown in Fig.16. It can be seen that JR-Takatori accelerogram inflicts much higher level of

damage in the structure than ITAJIMA accelerogram ( $D_{final}$  around 1.0). Still different combinations of  $\beta$  and  $c$  do not seem to cause much difference in the pattern of damage progression. Calculated damage indices under  $\beta=0.27$  are generally higher than those under  $\beta=0.11$ , and higher values of  $c$  make the damage index go lower.

While the displacement response is still cumulatively sensitive to the difference in  $c$  values, difference caused by different  $\beta$  values (under the same  $c$ ) seems to be more conspicuous than when under ITAJIMA accelerogram. This is possibly because of the higher damage level under JR-Takatori. Fig.17 shows responses under different  $\beta$  values with  $c=1.5$ . Fig.18 compares the responses under different  $c$  values with  $\beta=0.27$ .

The following conclusions may be drawn from this investigation: Structural responses vary with different values of  $\beta$  and  $c$ , and are especially sensitive to the value of  $c$ . And for the hysteretic model to realistically reflect the actual behavior of the structure, cautions should be taken in choosing the two free parameters.

## 8. Conclusions

To extend the damage-based hysteretic model for use with pipe-section steel bridge piers, a statistical approach is taken to determine the two free parameters— $\beta$ ,  $c$ . The role of  $\beta$  is to specify the relative importance of deformation based damage and plastic energy based damage; while  $c$  serves to link damage under general cyclic loading to damage under monotonic loading. It is found that with pipe-section steel bridge piers, it is adequate to fix  $\beta$  value at 0.27, and relate  $c$  to slenderness ratio  $\bar{\lambda}$  with a simple linear equation. Axial load ratio and radius-thickness ratio are found to have no significant influence on the free parameters. Thus through the systematic parameter identifying procedure, correlation between the free parameters and the structural parameters is clarified. In view of similarity of problems, relationship between the free parameters and the structural parameters is expected to be similar with box-section bridge piers although the specific values might be different.

Based on monotonic FEM analysis, other parameters of the hysteretic model are also given as functions of structural parameters. These efforts to determine model parameters culminate in simulation of pseudo-dynamic tests. Comparison of analytical and experimental results indicates the damage-based model is successfully extended to inelastic seismic response analysis of pipe-section steel bridge piers.

## Acknowledgements

The authors want to thank the joint research group of Public Works Research Institute, Tokyo Highway Association, Hanshin Highway Association, Nagoya Public Highway Corporation, Kozai Club Inc. and Japan Bridge Construction Institute Inc. for providing pseudodynamic test data used in this paper.

## Appendix : Monotonic loading parameters

Monotonic loading parameters of the damage-based

hysteretic model are:  $H_{max,1}$  (maximum strength),  $\delta_m$  (displacement corresponding to  $H_{max,1}$ ),  $\delta_u$  (displacement at collapse) and  $\alpha$  (ratio of strain-hardening stiffness to elastic stiffness). Based on monotonic  $H-\delta$  curves obtained from large-deformation inelastic FEM analysis, empirical equations for these parameters are given as follows:

$$\frac{H_{max,1}}{H_y} = \frac{[0.204(1+P/P_y)]^{4.87}}{(R_t^2 \bar{\lambda})^{0.8}} + 1.32 \quad (A1)$$

$$\frac{\delta_m}{\delta_y} = \frac{0.00064}{(R_t \sqrt{\bar{\lambda}})^{2.61}} + 1.04 \quad (A2)$$

$$\frac{\delta_u}{\delta_y} = \frac{0.037}{(1+P/P_y)^{2.5} R_t^{1.89} \bar{\lambda}^{-1.14}} + 1.15 \quad (A3)$$

$$\alpha = \left( \frac{0.081}{R_t} \right)^{3.93} \bar{\lambda}^{-0.01 R_t^{-2}} + 6.3 R_t - 0.1 \quad (A4)$$

And Eqs.(A1)-(A4) shall apply to  $0.10 \leq P/P_y \leq 0.30$ ,  $0.050 \leq R_t \leq 0.110$ ,  $0.20 \leq \bar{\lambda} \leq 0.50$ .

## References

- 1) S. Kumar and T. Usami: An evolutionary-degrading hysteretic model for thin-walled steel structures, *Engineering Structures*, Vol. 18, No.7, pp.504-514, 1996
- 2) T. Usami and S. Kumar: Inelastic seismic design verification method for steel bridge piers using a damage index based hysteretic model, *Engineering Structures*, Vol. 20, Nos4-6, pp.472-484, 1998
- 3) T. Kindaichi, T. Usami and S. Kumar: A Hysteresis Model Based on Damage Index for Steel Bridge Piers, *Journal of Structural Engineering, JSCE*, Vol. 44A, pp.667-678, March, 1998 (In Japanese)
- 4) S. Kumar, S. Mizutani, T. Okamoto: Nonlinear Dynamic Response of Thin Circular Steel Tubes, in 'Stability and Ductility of Steel Structures' edited by T. Usami and Y. Itoh, pp.319-326, Pergamon, 1998
- 5) S. B. Gao, T. Usami and H. B. Ge: Ductility Evaluation of Steel Bridge Piers with Pipe Sections, *Journal of Engineering Mechanics, ASCE*, Vol. 124, No.3, pp.260-267, 1998
- 6) ABAQUS/Standard User's Manual. (1996). Hibbit, Karlsson and Sorensen, Inc., Version 5.6, Vol. I & II.
- 7) C. Shen, Mamaghani I.H.P., E. Mizuno and T. Usami: Cyclic Behavior of Structural Steels. II: Theory, *Journal of Engineering Mechanics, ASCE*, Vol. 121, No.11, pp.1165-1172, 1995
- 8) Joint Research Report on Limit State Seismic Design of Highway Bridge Piers (VII), Public Works Research Institute, Tokyo Highway Association, Hanshin Highway Association, Nagoya Public Highway Corporation, Kozai Club, Inc. and Japan Bridge Construction Institute, Inc., 1997 (in Japanese)
- 9) Design Specifications of Highway Bridges (Part V. Seismic Design), Japan Road Association, December 1996

(Received September 18, 1998)